

Advances in high-throughput, high-capacity nonwoven membranes for chromatography in downstream processing: A review

Joseph Lavoie¹ | Jinxin Fan² | Behnam Pourdeyhimi^{2,3} | Cristiana Boi^{1,2,4}  | Ruben G. Carbonell^{1,2,5}

¹Biomanufacturing Training and Education Center, NC State University, Raleigh, North Carolina, USA

²Department of Chemical and Biomolecular Engineering, NC State University, Raleigh, North Carolina, USA

³Nonwovens Institute, NC State University, Raleigh, North Carolina, USA

⁴Department of Civil, Chemical, Environmental, and Materials Engineering, Alma Mater Studiorum-Università di Bologna, Bologna, Italy

⁵National Institute for Innovation for Manufacturing Biopharmaceuticals (NIIMBL), University of Delaware, Newark, Delaware, USA

Correspondence

Cristiana Boi, Department of Civil, Chemical, Environmental and Materials Engineering, Alma Mater Studiorum-Università di Bologna, via Terracini 28, 40131 Bologna, Italy.
Email: cristiana.boi@unibo.it

Funding information

William R. Kenan, Jr. Institute; Novo Nordisk Foundation, Grant/Award Number: #NNF19SA0035474

Abstract

Nonwoven membranes are highly engineered fibrous materials that can be manufactured on a large scale from a wide range of different polymers, and their surfaces can be modified using a large variety of different chemistries and ligands. The fiber diameters, surface areas, pore sizes, total porosities, and thicknesses of the nonwoven mats can be carefully controlled, providing many opportunities for creative approaches for the development of novel membranes with unique properties to meet the needs of the future of downstream processing. Fibrous membranes are already finding use in ultrafiltration, microfiltration, depth filtration, and, more recently, in membrane chromatography for product capture and impurity removal. This article summarizes the various methods of manufacturing nonwoven fabrics, and the many methods available for the modification of the fiber surfaces. It also reviews recent studies focused on the use of nonwoven fabric devices in membrane chromatography and provides some perspectives on the challenges that need to be overcome to increase binding capacities, decrease residence times, and reduce pressure drops so that eventually they can replace resin column chromatography in downstream process operations.

KEYWORDS

downstream purification, fibrous systems, membrane adsorbers, membrane chromatography, nonwovens, product capture and polishing

1 | INTRODUCTION

The biopharmaceutical industry is experiencing an increased demand for existing products to meet the needs of a growing global market, and international competition from the development of biosimilars is providing strong motivations to reduce costs. In addition, there is an increasingly diverse portfolio of new therapeutic modalities that

address a variety of diseases that must be produced at a wide range of process scales. These factors are contributing to the need for new devices and process approaches for biopharmaceutical development and manufacturing that reduce capital and operating costs, increase the flexibility of equipment and facilities to accommodate an evolving portfolio of products, and reduce both energy and water use (Erickson et al., 2021). There are several avenues that can be pursued

This is an open access article under the terms of the Creative Commons Attribution-NonCommercial-NoDerivs License, which permits use and distribution in any medium, provided the original work is properly cited, the use is non-commercial and no modifications or adaptations are made.

© 2023 The Authors. Biotechnology and Bioengineering published by Wiley Periodicals LLC.

to achieve this required transformation in biologics manufacturing, including the development of next-generation product capture and purification technologies that can handle process streams with high titers, increase productivity, have a smaller footprint, and involve single-use devices to reduce costs. Process intensification (PI) through semi-continuous and continuous processing can play a key role in achieving these goals, leading to a great deal of interest in the use of simulated moving bed (SMB) approaches, including rapid cycling or periodic counter-current chromatography technologies. Significant savings have been demonstrated by process conversions to single-use technology (SUT) from traditional hard-piped stainless steel reactor vessels and other equipment (Lopes, 2015). The use of SUT has been estimated to result in an over 20% reduction in cost of goods (COG) overall (Sinclair & Mange, 2009).

The need for increased productivity through higher binding capacity and faster processing times has placed a burden on resin column chromatography steps which, while capable of scaling to meet these needs, suffer from the high cost of chromatographic resins, necessary long residence times due to intraparticle diffusional resistances, high energy use for clean-in-place (CIP) procedures, and large buffer and footprint requirements (Fan et al., 2015; Vogg et al., 2020; Zydney, 2021). The need for process scale single-use devices that can operate at short residence times at moderate pressure drops, are simple to scale, and flexible enough to operate in a batch, semi-continuous or continuous mode has motivated the increased use of membranes to replace resin column chromatography in downstream product capture and purification steps (Davis et al., 2021; Trnovec et al., 2020).

For a long time, cast membranes, and some fibrous membranes, have been utilized in pressure-driven filtration steps such as depth filtration and microfiltration (MF) for cell harvest or cell debris removal, ultrafiltration (UF) for concentration steps, ultrafiltration/diafiltration (UF/DF) for buffer exchange, nanofiltration for virus or pathogen removal and reverse osmosis for ultrapure water production. The use of microporous membranes for chromatographic applications was introduced more than 40 years ago with the pioneering work of Elias Klein on affinity membranes (Klein, 1991). Since these membranes had very low binding capacity, it was thought to place them on top of each other so as to arrange them in layered stacks and form columns (Etzel, 2003; H.-C Liu & Fried, 1994). Due to their low capacity, cast membranes have also been commonly used in a flow-through or frontal mode for product polishing by removing product and process impurities after the product capture step (Nadar et al., 2022; Trnovec et al., 2020; Vogg et al., 2020). However, the use of membranes in a bind-and-elute mode for product capture and purification is not common since the relatively low surface area of cast membranes when compared with traditional chromatography resins limits their maximum binding capacity. Consequently, bind-and-elute operations using cast membranes require a very large number of rapid cycles to treat a whole batch and result in dilute product streams and large amounts of buffer use.

In recent years, both industrial and academic groups have made significant progress in the development of high-capacity product

capture membranes based on nonwoven fabrics whose surfaces are modified with ion exchange, affinity, and salt-tolerant ligands. These membranes, like other membrane devices, are suitable for single-use operation with short residence times and are easy to scale up and to integrate into a production line.

This review article describes the various methods and materials used to manufacture nonwoven fabrics, their physicochemical characteristics, and fiber surface modification approaches for their use in downstream purification of biologics. Examples of academic and commercial efforts to use these membranes for the capture and polishing of biologics from cell culture media are described and compared. There are several examples of membrane applications with a wide variety of biomolecules, from relatively small proteins such as lysozyme, to monoclonal antibodies, but it is with large molecules, such as viruses, nucleic acids, and cells, that these membranes offer the greatest advantages over column chromatography (Boi, 2018). This field is still in relative infancy, and an argument can be made that the properties of these membranes can enable entirely new process approaches for more flexible and efficient high-productivity downstream processes.

2 | USE OF MEMBRANES IN DOWNSTREAM PROCESSES

Traditionally, porous chromatographic resins have been the medium of choice for product purification in downstream processing applications. Composed of a variety of materials, including porous silica, cross-linked agarose, and poly(methyl methacrylate) (PMMA), resin selection depends on a number of factors such as particle diameter, pore size, ligand properties, binding capacities for product or impurities, binding, buffer utilization, cleaning-in-place, and storage conditions. These porous substrates are available with a wide range of ligands: ion exchange, hydrophobic interaction, affinity, multimodal, and they enable highly customized purification processes resulting in product streams that meet stringent safety, efficacy, and quality standards.

Preparative chromatography columns use relatively large diameter particles (40–60 μm) to reduce pressure during flow and have volume fractions of about 0.40–0.45. As a result, the hydraulic diameters of channels available for flow between particles are approximately 1/9 to 1/7 of the particle diameter, or 7–8 μm for a bed packed with 60 μm particles according to the equation (Bird et al., 2001),

$$d_h = D_p \epsilon / 6(1 - \epsilon). \quad (1)$$

Because of the relatively large particle diameters, the residence times must be on the order several minutes to allow diffusion into the particles. To maintain low-pressure drops at these residence times, column lengths are normally kept at values less than 25 cm and the column size can be scaled up by increasing the diameter of the column. The main advantage of chromatographic resins is their

capacity, which can reach values of more than 100 mg of protein per mL of resin for ion exchange. Proteins larger than antibodies or biologics, like viral vectors, oligonucleotides, and plasmids, are too large to penetrate the pores of most chromatographic resins (1000 Å for mAb purification), reducing the effective binding capacity for these products. Lastly, resins are expensive and, as a result, even if all other barriers to their use in process intensification efforts were removed through significant advances in resin technology, the base material still would be economically prohibitive for single-use applications (Rathore et al., 2018).

Most of the membranes used currently for bacterial and viral removal, ultrafiltration, microfiltration, and nanofiltration are polymeric membranes made by *immersion casting* (cast membranes). In this process, the polymer to be cast is dissolved in a solvent and extruded into a coagulation bath. The bath is filled with a nonsolvent liquid, such as water, inducing a phase separation of the polymer solution. This phase separation yields solvent-rich and polymer-rich regions which form the pores and membrane respectively (Galiano, 2020). The structure of these materials can be very finely tuned through manipulation of the polymer concentration, additive concentration, solvent, and nonsolvent selection, and bath temperature, among others (Kim et al., 2010; Nevstrueva et al., 2018; Son et al., 2014). A similar process is also used for the production of hollow fiber membranes often utilized in crossflow ultra- and micro-filtration applications (Wood et al., 1993).

Though the highly uniform pore structures of cast membranes are advantageous for their ability to generate high-purity filtrate streams with tunable molecular weight limits and relatively high permeabilities compared to packed bed resin systems, the intrinsic surface areas of these materials are typically orders of magnitude lower than porous resin analogues. For example, Figure 1 shows the structure of the Sartobind[®] S cation exchange cellulose cast membrane compared to a regenerated cellulose nanofiber adsorbent and a Fractogel EMD TMAE HiCap chromatography resin with 40–90 μm particle size and 0.1 μm (1000 Å) pore size. The cation exchange cast membrane has pore sizes of about 5 μm compared with the

nonwoven membrane whose fiber diameters seem to be less than 1 μm and pore diameter around 2–3 μm. The hydraulic diameter of a column packed with these resins would be approximately 8–10 μm, and the internal surface area of the particle would be approximately 50 m²/g.

Still, there are substantial advantages for the use of membranes when functionalized for different modes of separation, especially if high binding capacities can be achieved. For one, the binding kinetics are favorable since there are no diffusional limitations to adsorption other than through the very thin hydrodynamic binding layer along the surface of the membrane pores (Orr et al., 2013). This allows for faster bind and elute cycling, yielding significant gains in productivity. Depending on dynamic binding capacity of the membrane, it may or may not need further concentration steps after product capture and elution. In addition, the large pores provide easy access for large species such as viral vectors, oligonucleotides, and plasmids and allows for the same membrane to be used for purification of different biologics.

It is evident from this discussion that the ideal membrane device should take advantage of the large pore diameters and high porosity of the membrane and have as high a binding capacity as possible to handle streams with high titers, increase productivity and eliminate the need for post-elution product concentration. Higher binding capacities can be achieved by increasing the surface area of the membrane pores and by grafting polymeric coatings on the surface to enhance binding capacity beyond the monolayer coverage on the pore surface. For this purpose, many researchers have turned in recent years to the use of nonwoven fabrics as membranes for these applications. This has led to two major innovations in nonwoven membrane development: production methods for webs of sub-micron fibers for larger surface areas, and surface grafting of polymer coatings which can significantly increase the binding of biologics. The sections that follow describe the wide array of techniques that are available to make nonwoven fabrics, and the numerous opportunities these provide for the development of the next generation of high-capacity, high-productivity membrane-based chromatography supports for downstream processing.

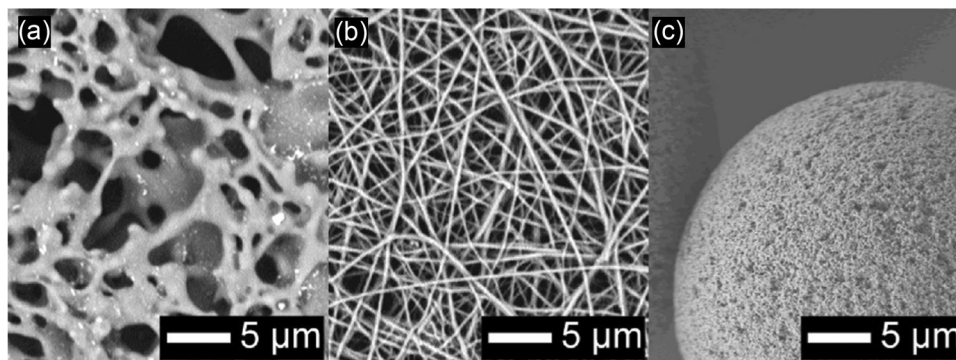


FIGURE 1 Scanning electron microscope images: (a) Cast Sartobind[®] S cellulose membrane; (b) Cellulose nanofiber adsorbent; (c) Fractogel[®] EMD TMAE HiCap resin with 40–90 μm diameter and ~0.1 μm pores (Dods et al., 2015).

3 | NONWOVEN MEMBRANES: METHODS AND PROPERTIES

3.1 | Nonwoven fabrication

Nonwovens are highly engineered web structures that are formed directly from a wide variety of natural or man-made fibers starting with either solid thermoplastic polymer pellets or powders or pre-cut polymer staple fibers (Batra & Pourdeyhimi, 2012). These materials can be manufactured under GMP conditions to very high standards of quality and consistency. Figure 2 shows the *manufacturing toolbox* that is currently available for nonwoven fabric production, from raw material to polymer preparation, web formation, and bonding.

Many of the membranes that have been used for downstream applications are manufactured beginning with polymeric particles that are dissolved using an appropriate solvent then passed through a nozzle under an electric field onto a moving belt. This process is called *electrospinning*, where the fiber diameter and other membrane properties can be controlled by the magnitude of the electric field, the polymer solution concentration and flow rate, and the basis weight, or area density (g/m^2), is controlled by belt velocity (Long et al., 2019). This process is popular for nonwoven membrane formation because it can be used with any polymer that has a suitable solvent, and results in sub-micron ($< 0.5 \mu\text{m}$) fiber diameters. Compared to other web formation techniques, electrospinning has a much lower throughput in terms of membrane production, and the small fiber diameters result in webs that have poor mechanical properties and small pores that can decrease the flow permeability. Thus, sub-micron fiber diameter membranes are normally thinner to maintain the overall pressure at reasonable values under flow.

Other investigators have used nonwoven fabrics made by a process called *meltblowing*, in which molten polymer is introduced into dies with numerous nozzles through which the polymer is

extruded while two very high velocity converging hot air jets are introduced along the direction of polymer flow to help stretch the fibers. The fibers undergo bending stability, start whipping and touch neighboring fibers and form a self-bonded web. This is very similar to electrospinning except that the aerodynamic forces are responsible for fiber stretching (Pinchuk et al., 2012). The fiber diameter, membrane pore size, overall porosity, and the basis weight, which correlates with the membrane thickness, can all be controlled through the manipulation of process variables such as extrusion throughput and temperature, air flow velocity and temperature, belt speed and the distance from the die to the collector. Depending on the viscosity of the polymer and the process conditions, it is possible to achieve fiber diameters with a broad size distribution in the range of $0.5\text{--}5.0 \mu\text{m}$, but by careful control of the polymer flow and air jet system, fibers as small as 36 nm have been obtained (Soltani & Macosko, 2018).

Meltblowing, as a roll-to-roll process, has a much higher throughput than electrospinning, and it does not require solvents. It is used to create nonwovens for very high-volume applications, including air filtration media, masks and respirators, hospital gowns, napkins, and wipes in single machines that are over 15 feet in width and move at high velocity. Membranes with fiber diameters in the range of $1\text{--}3 \mu\text{m}$ are more mechanically stable, have larger pores, and have higher flow permeabilities than those with sub-micron fibers. However, the fiber diameter distribution of nonwovens made by meltblowing are wider than those made by electrospinning. Because of their larger fiber diameters meltblown fabrics do have lower surface areas than electrospun materials, but as we will see later, this can be overcome by using optimized grafting conditions. Meltblowing is commonly used to make nonwovens from polyolefins like polypropylene (PP) and polyethylene (PE); polyesters such polybutylene terephthalate (PBT), polyethylene terephthalate (PET), polylactic acid (PLA) and polycarbonate; polyamides including Nylon 6, 11 and 12; polymethyl methacrylate

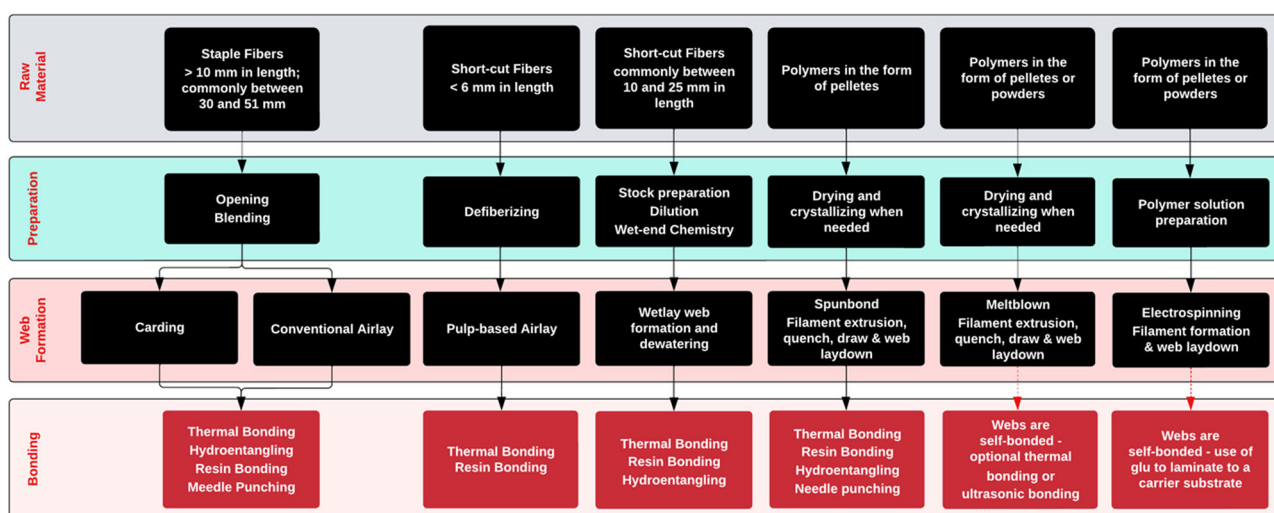


FIGURE 2 Toolbox for manufacturing nonwoven fabrics from both polymer powders and pellets as well short-cut ($< 6 \text{ mm}$ length) and staple polymer fibers ($> 10 \text{ mm}$ length).

(PMMA); and fluorinated polymers such as polyvinylidene fluoride (PVDF) and polytetrafluoroethylene (PTFE).

Spunbonding is a process that resembles *filament extrusion*, but in this case the filaments are drawn by high-velocity air; the air also randomizes the web laydown before landing on the moving belt. This process results in fiber diameters in the 15–35 μm range for most applications using a spunbond fabric, and much thicker membranes with larger basis weights. The fiber diameter distribution is extremely narrow, and the structures are generally uniform. Large fiber diameters are possible, but it is difficult and not economically feasible to produce fibers smaller than 15 μm by using a standard homo-component fiber. Smaller fibers become feasible when using a bicomponent fiber as will be discussed later in this section. There are many polymers that are used in spunbonding, including PP, PET, polyamides, PBT, PLA, and Polytrimethylene terephthalate (PTT).

As can be seen from Figure 2, the approaches used to make nonwoven webs from short-cut fibers (less than 6 mm to 25 mm in length) and staple fibers (30–50 mm in length) involve *Carding*, *Airlay* or *Wetlay* approaches where the fibers are mechanically separated (carding) suspended, either in air (airlay) or in aqueous suspensions (wetlay) respectively, and passed through rotating belts or cylinders that capture the fibers (Batra & Pourdeyhimi, 2012). In this case, the fiber diameter is determined by the fiber materials used, but the thickness, porosity, and basis weight of the membrane are controlled by the concentration of fiber, any additives present, the air or liquid flow rate to the collector, and the collector velocity. This type of process can be used to manufacture depth filters that combine more than one type of fiber or a mixture of fibers and particles. It can also be carried out as a continuous or batch process depending on the required volume of nonwoven webs required.

It should also be noted in Figure 2 that there are numerous bonding methods that can be used after the web formation step to improve the membrane's mechanical properties and integrity. This can be done mechanically, thermally, or chemically. Mechanical bonding is done using needles (needle-punching) or water jets (hydroentanglement) that induce fiber–fiber entanglements to enhance the strength of the fabric. Thermal bonding causes fibers to adhere to each other and is achieved by thermal calendaring (due to heat conduction), or hot air impingement (due to heat convection).

Finally, it is common to spray or foam small amounts (less than 10%) of adhesive materials on the fabric to help bond fibers in the nonwoven to achieve further strength of the web.

There are also technologies available for the extrusion of *bicomponent* fibers to take advantage of the differences in mechanical and chemical properties of the two individual polymers to enhance the performance of the nonwoven. Figure 3 shows cross-sections of various fiber extrusions that comprise two different polymers. Once the web is formed, the two polymers can be split and entangled to obtain stronger nonwovens, or they can be used to create self-crimping fibers if the two polymers have different shrinkage or elastic properties. The *Islands-in-the-sea* configuration in Figure 3 can be used with a soluble polymer like PLA in the continuous phase (the sea) and an insoluble polymer like PBT as the islands so that after web formation dissolution of the sea will leave behind fibers of the island that are 1 μm or less. Several patents cover the manufacturing of islands-in-the-sea structures (Pourdeyhimi & Sharp, 2011; Pourdeyhimi et al., 2013a, 2013b) and a patent on the conformal grafting of islands-in-the-sea nonwoven fabrics was issued to Heller et al. (M. Heller et al., 2021). Finally, complex fiber cross sections can also be extruded to increase the surface area of a fiber beyond its nominal diameter. Figure 4 shows a picture of a “multi-lobed” or “winged” fiber as an example of such a configuration. The winged fiber technology was developed by B. Pourdeyhimi and W. Chappas, and is protected by several patents (Chappas & Pourdeyhimi, 2013; Pourdeyhimi & Chappas, 2012; Pourdeyhimi et al., 2016); while a patent for the use of these high area fibers for downstream processing has been issued to Gurgel et al. (Gurgel et al., 2012).

The fiber diameter plays a key role in determining many of the most important physical properties of the nonwoven membrane. The porosity ϵ of most nonwovens is generally in the range of $0.7 < \epsilon < 0.9$. The surface area of fibers per unit volume of membrane a_f is easily estimated for circular fibers to be,

$$a_f = (1 - \epsilon)4/d_f \quad (2)$$

As expected, the surface area increases proportionally as the fiber diameter decreases. If the only mechanism for adsorption is the

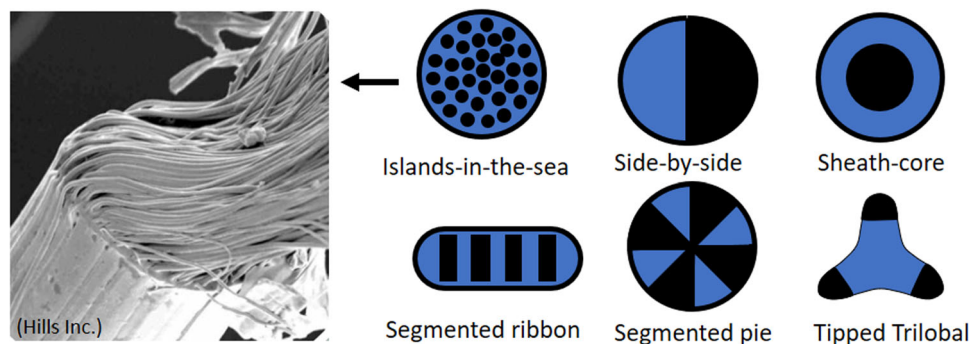


FIGURE 3 Cross-sections of *bicomponent* fibers extruded with two different polymers shown in different colors (blue and black).

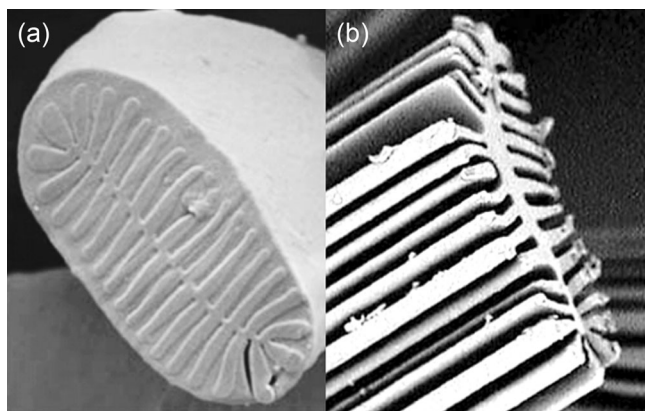


FIGURE 4 Multilobed (winged) bicomponent fiber with external sacrificial polymer (a), and the resulting multi-lobed or winged fiber formed of the internal polymer after removal of the sacrificial component (b). (Allasso Industries, Inc.).

formation of a monolayer of product, say proteins, on the surface, the binding capacity would be directly proportional to a_f . If the target species is much larger than the fiber diameter, it might lead to decreased passage through the membrane and lower accessibility. The average pore diameter in the nonwoven can be roughly estimated by the equation (Goeminne et al., 1974),

$$d_p = d_f / (1 - \epsilon). \quad (3)$$

As the fiber diameter decreases the pore diameter also decreases proportionally. Figure 5 shows the increase in surface area per unit volume of fiber and the decrease in pore size as the fiber diameter decreases. Decreased pore size will contribute to a reduction in the pore size cut-off of the device, which would potentially be a design consideration for products with especially large hydrodynamic radii, though generally the pore sizes for nonwoven membranes are several microns, and orders of magnitude larger than most molecules of interest. Most significantly, smaller pores lead to increased tortuosity of flow paths, which can have an important effect on the flow permeability k in Darcy's Law as applied to a nonwoven,

$$v = k \frac{\Delta P}{\mu L}. \quad (4)$$

This equation relates the superficial velocity v of fluid flowing through the nonwoven to the pressure drop per unit length (depth) of membrane $\Delta P/L$ and the fluid viscosity μ . There are numerous correlations indicating that the relative permeability varies as the square of the fiber diameter, such as shown below by Davies (Davies, 1953),

$$k = \frac{d_f^2}{64a^2(1 + 56a^3)}. \quad (5)$$

Here a is the solid volume fraction ($1 - \epsilon$). The permeability of nonwovens is usually expressed in units of Darcy (Da) where 1 Da is

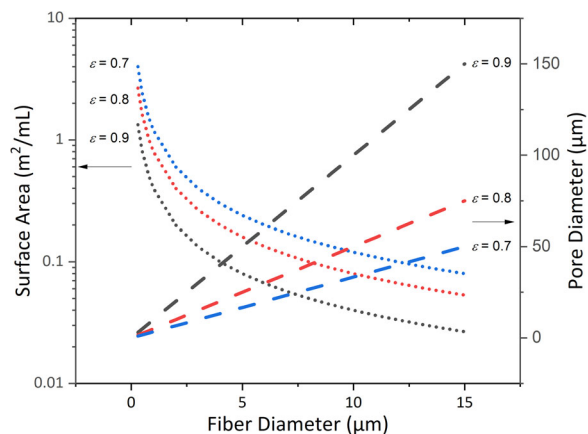


FIGURE 5 Effect of fiber diameter on nonwoven membrane area and nominal pore size based on estimates from Equations (2) and (3), respectively.

approximately 10^{-12} m^2 . Darcy's Law in Equation (4) can be rearranged to calculate the thickness L of a nonwoven membrane that can operate at a fixed maximum pressure drop ΔP as a function of residence time $\tau = L/v$ with a fluid with a viscosity μ close to that of water

$$L = \sqrt{k \frac{\Delta P \tau}{\mu}}. \quad (6)$$

Figure 6a shows the expected decrease in permeability as the fiber diameter decreases, and Figure 6b illustrates the diminution of the maximum membrane thickness achievable as you decrease the residence time in the membrane at fixed pressure drop (8 bars in this case). The smaller membrane thicknesses are problematic since the thinner the membrane, the larger the number of membrane stacks needed to be used in parallel to handle large volumes of supernatant. This could increase capital costs, and buffer use, and result in dilute product recovery.

In summary, reducing the fiber diameter can increase the binding proportionally, but it also raises the pressure drop at a given flow rate more strongly. This can limit the residence time during operations, or the membrane thickness required for a desired residence time at a given operating pressure. In the paragraphs that follow we will discuss various approaches to the functionalization of nonwoven fibers to enable use in downstream processing. It needs to be pointed out that grafted layers of charged hydrogels can also affect the flow permeability significantly due to grafted layer expansion due to charge repulsion effects at low ionic strength and grafted layer contraction of high ionic strength.

3.2 | Nonwoven functionalization

The surface of the fibers in nonwoven membranes that are to be used for bioprocessing need to be modified to achieve three goals: (1) hydrophilize the surface to prevent non-specific binding of proteins

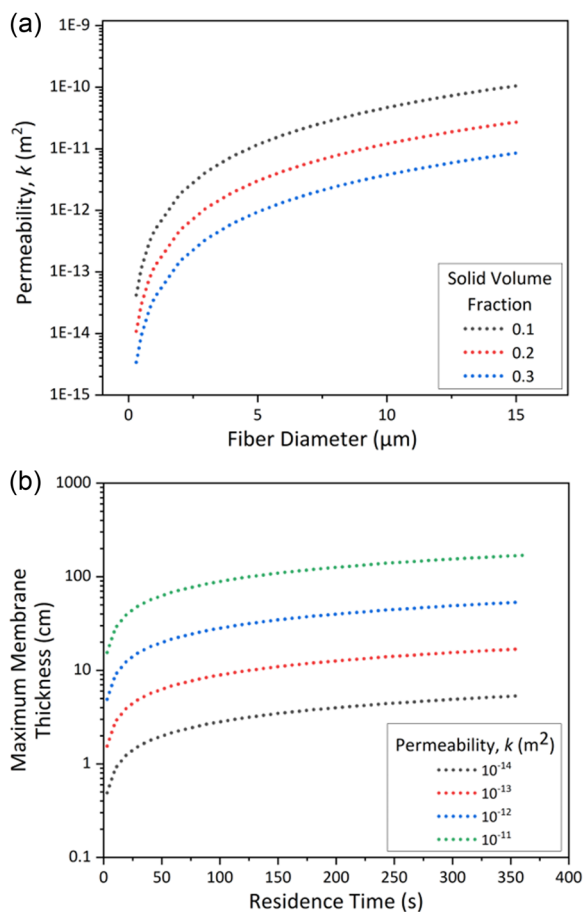


FIGURE 6 (a) Effect of fiber diameter on flow permeability based on Equation (5); (b) Effect of flow permeability on the maximum filter thickness allowable as a function of desired residence time at fixed pressure drop of 8 bar based on Equation (6).

and other contaminants to increase yield and purity; (2) impart the necessary functionality for the desired operation, be it ion exchange, salt tolerant or multimodal ligands, or affinity ligand; and (3) increase the adsorption capacity. Some of the approaches used to reach these goals involve “grafting from” polymerization of hydrogels to the fiber surface to render it hydrophilic. These grafted layers often serve to create relatively thick regions into which product molecules or impurities can diffuse and significantly increase the binding capacity relative to the small capacities that would result with just monolayer coverage. There is a huge body of literature on the various methods that can be used to chemically modify polymer fiber surfaces. Sun et al. (Sun et al., 2020) divide these into two approaches: “grafting to” in which a polymer is attached to the surface of the fiber after activation, and “grafting from” to describe the formation of compact polymer aggregates (mushroom or pancake shaped) or stretched polymeric brushes from a surface that has been coated with initiators and monomers in solution. UV-, and heat-induced grafting has been used to form poly(glycidyl methacrylate) (pGMA) on the surface of PP and PBT for the attachment of a variety of ligands through the

pendant epoxy groups. An often-used approach for fiber modification is surface-initiated atom-transfer radical polymerization (SI-ATRP) catalyzed by surface-initiated halide groups and Cu and other metal catalysts. ATRP can be used with many monomers and initiators, and it leads to polymers with low polydispersity index and endings that can be easily functionalized. The main disadvantages are the need for a very high concentration of catalyst, which consist of copper halides and amine-based ligands, the requirement that reactions must be carried out under a nitrogen blanket, and the copper and halide need to be washed extensively after grafting before use of the membrane.

Table 1 lists some recent examples of approaches used to functionalize fibers for downstream applications. One of the strategies involves the formation of bicomponent fibers so one of the fiber components serves as a support matrix and the second has the necessary functionality to bind biological targets so there is no need for additional fiber surface coatings or modifications (Najafi et al., 2018; Yang et al., 2022). Another option is to *crosslink* a polymer that has the desired functionality to the surface of the nonwoven fibers, as was done by Cheng et al. (Cheng et al., 2022) in attaching polyethyleneimine to polyethylene-co-vinyl alcohol fibers. There are several examples shown in the table in which the polymer is reacted with small molecules, such as dyes or metal ions, without the presence of a grafted layer. This approach is simpler but relies completely on the adsorption capacity available on the surface of the fibers. Finally, there are several examples where hydrogels are polymerized in “grafted from” approaches as described above.

There are various ways of creating pGMA hydrogels on fiber surfaces, Schwellenbach et al. (2016), reacted winged PET fibers with polyallyl amine to introduce a high concentration of amines on the surface. These were then reacted with bromoisobutylbromide (BiBB) to add a halide group (Br) on the surface that enables the use of SI-ATRP by reacting with GMA in the presence of Cu(I)Br. On the other hand, Winderl et al. (2021) modified physically similar winged fibers of polyamide 6 (PA6) using a cerium (IV) nitrate (ACN)-initiated grafting via free radical polymerization of GMA in the presence of methylenebisacrylamide without any specific surface initiation. Zheng et al. (2010) grafted GMA on PP by first exposing the bare PP to UV light at 185/254 nm wavelength in air to create radical groups on the surface. After that, they used UV-initialized free radical polymerization of GMA at 365 nm with benzophenone as photoinitiator. The degree of grafting was dependent on the time of exposure to light. Heller et al. (2020) grafted GMA on PBT using two different approaches: (1) UV-induced grafting of GMA using benzophenone at a wavelength of 365, without the need for UV pretreatment to generate radicals; (2) Heat-induced grafting where the nonwoven was first dipped in the thermal initiator benzoylperoxide, and then introduced into a GMA solution and heated. Both approaches led to the same weight gain of grafting of pGMA, but they had very different properties. The heat-induced samples had a smaller binding capacity, and they did not exhibit the slow approach to equilibrium shown by the UV-grafted materials. In addition, the heat-induced samples exhibited size selectivity so that smaller molecules had a higher molar equilibrium binding capacity than

TABLE 1 Polymers used in studies on nonwoven fabrics for chromatography, methods for surface modification, and ligands and interactions used for the adsorption of biologics.

Membrane	Surface modification	Ligand	Reference
PBT	UV- and Heat-induced grafting of glycidyl methacrylate	Sulfonate (CEX), Diethylamine (AEX), Triethylamine (AEX), Iminodiacetic acid (CEX), 2-mercaptopyridine-3-carboxylic acid (MPCA)	Heller et al. (2020); Lemma et al. (2021); Fan et al. (2021); Fan et al. (2022); Fan et al. (2023)
Cellulose	Cerium Ammonium Nitrate (CAN) polymerization of acrylonitrile	Polypropionic acid (CEX), Polyethyleneamidoamine (AEX)	Rajesh et al. (2017); Rajesh et al. (2018)
Polyolefin	Polyacrylamide hydrogel (Natrix Q)	Quaternary amine (AEX)	Hou et al. (2015)
Polyolefin	Polyacrylate hydrogel (Natrix)	Carboxylate (CEX)	Hassel and Moresoli (2016)
PET	SI-ATRP of glycidyl methacrylate	Sulfonate (CEX)	Schwellenbach et al. (2016)
Regenerated cellulose	UV grafting of 4-vinylpyridine	Cu ²⁺ (metal chelation)	Amaly et al. (2020)
Nylon 6 fibers	Reaction with citric acid via EDC	Cu ²⁺ (metal chelation)	Amaly et al. (2020)
Polyvinyl alcohol-co-ethylene fibers	Reaction with sodium-3-sulfobenzoate via EDC	Sulfonate (CEX)	Amaly et al. (2018)
Regenerated cellulose	ATRP grafting of N-vinylcaprolactam monomer	N-vinylcaprolactam (hydrophobic interaction)	Cheng et al. (2022)
Polysulfone and Polyacrylonitrile	UV grafting of glycidyl methacrylate	Diethylamine (AEX)	Chen et al. (2020)
Cellulose acetate	Ring-open reaction with phenyl glycidyl ether using BF ₃ ·Et ₂ O as catalyst	Phenyl (hydrophobic interaction)	Wang et al. (2019)
Ethylene vinyl alcohol	Reaction with butane tetracarboxylic acid - polyphosphoric acid as catalyst	Carboxylate (CEX)	Fu et al. (2019)
Ethylene vinyl alcohol	Reaction with citric acid using polyphosphoric acid as catalyst	Carboxylate (CEX)	Fu et al. (2016)
Regenerated cellulose	Reaction with cyanuric chloride and iminodiacetic acid	Metal chelated Fe ³⁺	Duan et al. (2018)
SiO ₂ /SnO ₂ nanofibers	Hydrogel formed by dip-coating in citric acid and polyvinyl alcohol (PVA)	Carboxylate (CEX)	Fu et al. (2022)
Regenerated cellulose	Direct coupling	RO4 dye	Jian et al. (2022)
Ethylene vinyl alcohol	Polyethyleneimine (PEI) and glutaraldehyde crosslinked matrix	Polyethyleneimine (AEX)	Cheng et al. (2022)
Bicomponent fibers of PAN ^a and pAQ ^b	No additional fiber surface coating	Quaternary amine (AEX)	Yang et al. (2022)
Bicomponent fibers of PVA ^c and PMA ^d	No additional fiber surface coating	Carboxylate (CEX)	Najafi et al. (2018)
Ethylene vinyl alcohol co-polymer	Crosslinked matrix with polyethyleneimine (PEI) and glutaraldehyde	Polyethyleneimine (AEX)	Cheng et al. (2022)

^aPolyacrylonitrile.

^bRAFT copolymerized acrylonitrile and DMAEA.

^cPVA, polyvinyl alcohol.

^dPMA = poly(MVE/MA) = poly(methyl vinyl ether-alt-maleic anhydride) = poly(MVE/MA).

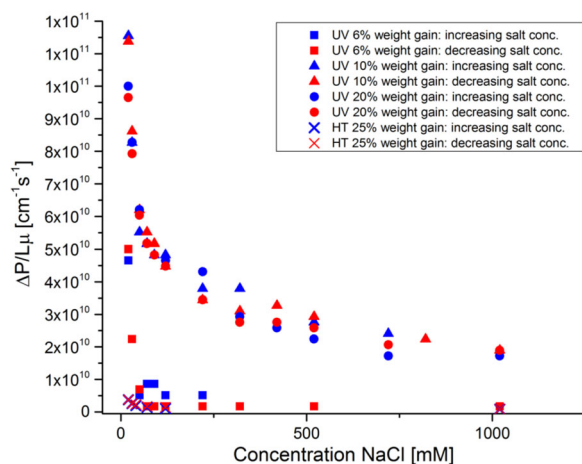


FIGURE 7 Pressure drop as a function of salt concentration at a fixed superficial velocity of 1.3 cm/min for PBT nonwovens grafted with GMA and functionalized with DEA for AEX using both UV- and Heat-induced grafting. UV-grafted membranes had weight gains of 5%, 10%, and 20%; Heat-induced grafted membranes had weight gains of 25% (Heller, M. Polymer grafted nonwoven membranes for bioseparations, Ph.D. Thesis, NC State University, 2015). DEA, diethylamine; GMA, glycidyl methacrylate; PBT, polybutylene terephthalate.

larger molecules. This evidence indicates that the heat-induced samples had less flexible, thinner grafted layers on the fiber surface. As opposed to the UV-grafted layers, the heat-induced layers were not as visible by SEM. As a good example of the strong effects of conductivity on flow permeability, Figure 7 shows the pressure drop at a fixed superficial velocity measured while increasing and decreasing salt concentrations. It is evident that (1) increased salt reduces the pressure drop; (2) the larger the ligand density (weight gain of grafted layer) the stronger the effect of salt, and (3) heat-induced grafted layers are much more rigid than UV-grafted layers and the effect of salt on their flow performance is not nearly as strong (M. L. Heller, 2015). The chosen nonwoven functionalization pathway plays a key role in the performance of the membrane, and it can greatly affect the time, effort, and environmental impact of its manufacture.

All these chemistries and more have been utilized for the creation of membrane-based bioseparations devices. As has been discussed, each method has advantages and disadvantages that can influence their selection depending upon various factors including the base material, the target to be captured, the presence or absence of heavy metal catalysts or toxic ions, and the number of steps used in membrane fabrication and functionalization. The sections that follow will discuss recent examples of these approaches to the development of nonwoven fabrics as membranes for downstream processing that have the specific goal of playing the same role as columns, namely, to operate in a bind-and-elute mode for product capture and to be used in a flow-through mode for polishing. Particular attention will be paid to work that has been done in this area that includes testing of the membrane materials under flow conditions that are close to those

encountered in biopharmaceutical processing operations, including representative product targets in complex supernatants from cell culture fluids, and where dynamic binding capacities, yields, purity, and other important factors have been determined.

4 | MELTBLOWN NONWOVENS

In our group at North Carolina State University, a platform was developed to produce high-capacity, high-throughput single-use membrane adsorbers from nonwoven fabrics. Initially, meltblown PP was used as the base material, but it required UV pretreatment before adsorption of the photoinitiator (Zheng et al., 2010, 2011). Therefore, it was abandoned in favor of commercial polybutylene terephthalate (PBT) nonwoven fibers with 3 μm average diameter, specific surface area of 0.8 m^2/g and void fraction of 80%, which is the material used in all subsequent work. GMA has been grafted onto fibers by both heat-induced grafting (M. Heller et al., 2020) and UV grafting (Fan et al., 2021, 2022; Lemma et al., 2021; H. Liu et al., 2015; W. Liu et al., 2005) before functionalization with various ion-exchange ligands.

In addition, fundamental studies on mass transfer limitations were performed using an islands-in-the-sea PBT with small fibers with an average diameter of 1 μm and a commercial PBT with larger fibers with a diameter of 3 μm . Both nonwovens were successfully grafted with pGMA and functionalized as weak anion exchangers using diethylamine (DEA) and strong cation exchangers by attaching phosphoric acid groups. For similar values of pGMA % weight gain, the membranes were endowed with approximately the same static binding capacity, about 150 mg/mL of BSA for AEX and 200 mg/mL of IgG for CEX (M. Heller et al., 2016). However, membranes prepared from smaller fibers showed fewer diffusive limitations than membranes prepared from larger fibers that require a thicker grafted layer because of their lower surface area. From a practical point of view, materials with smaller diameter fibers are more difficult to handle in the laboratory, especially when they need to be packed into columns for use in flow experiments. Work is being done to optimize these materials to ensure good flow properties and performance under dynamic conditions.

A side-by-side comparison between heat-induced and UV grafting revealed that UV-grafted membranes have a much larger static binding capacity, about 5 times for AEX and 7 times for CEX, than their heat-grafted counterparts as reported in Table 2 (M. Heller et al., 2020). The reason is likely due to the different structures of the grafted layers: UV grafting creates a pGMA structure that can accommodate more protein binding than the pGMA structure obtained using a heat-induced grafting approach, as can be observed from the SEM images and from the schematics shown in Figure 8a,b. This is also evident with the binding kinetics: the heat-induced grafted membranes achieved equilibrium on the order of minutes, while UV-grafted membranes required more than 10 h. Therefore, the ideal type of grafting might be chosen according to the specific application and to the size of the target molecule. Since the main goal

TABLE 2 Comparison of binding capacity for PBT nonwoven membranes prepared by UV and Heat grafting (data from Heller et al., 2020).

IEX type/protein bound	UV-grafted PBT polyGMA grafting			Heat grafted PBT polyGMA grafting		
	(% weight gain)	K_d ($\times 10^{-6}$ M)	q_m (mg/g)	(% weight gain)	K_d ($\times 10^{-6}$ M)	q_m (mg/g)
Anion exchange/BSA	14	3.0	771	15	1.4	30
Anion exchange/BSA	18	6.7	833	25	7.5	85
Cation exchange/hIgG	14	6.8	339	15	2.7	71
Cation exchange/hIgG	19	11.4	692	25	9.7	202

Abbreviations: GMA, glycidyl methacrylate; PBT, polybutylene terephthalate; UV, ultraviolet.

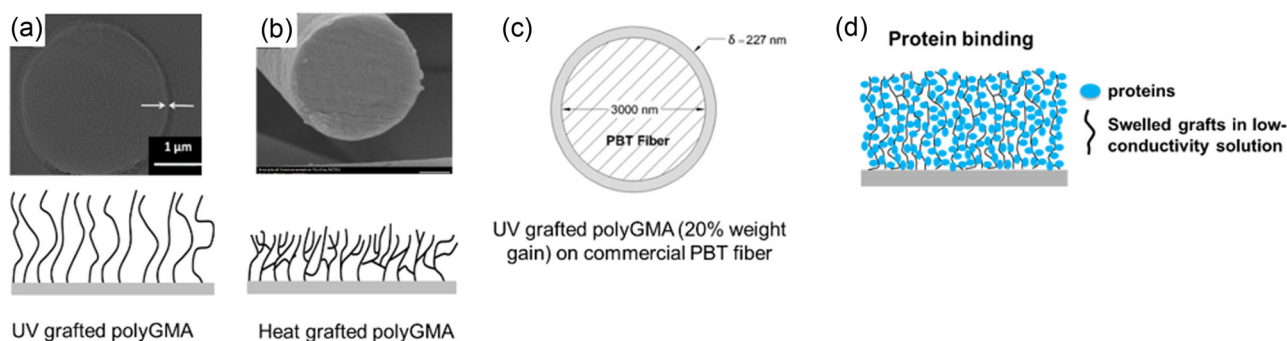


FIGURE 8 SEM images of pGMA grafted PBT fiber cross sections using UV (a) and using heat-induced grafting (b), both with grafted weight gains of 20%; (c) shows the estimated dimensions of the UV-grafted layer relative to the average fiber diameter. The large binding capacities at low ionic strength are likely due to hydrogel expansion allowing multilayer adsorption of proteins, as shown in (d) (Heller et al., 2020). GMA, glycidyl methacrylate; PBT, polybutylene terephthalate; SEM, scanning electron microscope; UV, ultraviolet.

is to develop materials to produce high-capacity, single-use membrane adsorbers for biopharmaceutical manufacturing, most recent work has focused on optimizing UV-grafted membranes. In general, the membrane binding capacity increases as ligand density increases, but 20% weight gain provides the best compromise between maintaining good permeability to flow and achieving high capacity (Lemma et al., 2021). The thickness of the grafted layer is about 200 nm at 20% weight gain of pGMA as depicted in Figure 8c, and the swelled charged grafts on the ion exchange membranes in the low conductivity buffer dramatically increased binding space/volume (Figure 8c), resulting in significantly larger binding capacity (nearly 1000 mg/g) than the 4–6 mg/g expected from monolayer coverage on 3.0 μm diameter fibers (M. Heller et al., 2016; Lemma et al., 2021). Several ligands have been successfully immobilized on the PBT base nonwoven matrix: diethylamine (DEA) weak anion and iminodiacetic acid (IDA) weak cation exchangers; triethylamine (TEA) strong anion and sulfonic acid (SO_3) strong cation exchangers; as well as salt tolerant ligands (under patent application). Salt tolerant ligands have been shown to exhibit high binding capacities at short residence times as listed in Table 1 (Fan et al., 2021, 2022, 2023; Lemma et al., 2021) and used in laboratory scale experiments to purify real cell culture fluids.

For example, the CEX- SO_3 membrane exhibited a very high binding capacity of 145.0 mg/mL at 0.1 min residence time for capturing polyclonal IgG from CHO supernatant achieving high HCPs

log removal value (LRV) of 1.2 and DNA removal of 1.9 LRV (Lemma et al., 2021). The productivity of membrane chromatography was estimated to be at least 10 times higher than resin chromatography. Fan et al. reported that the CEX-IDA membrane can be reused for five bind-elute cycles in capturing a real mAb from cell culture harvest at 1.0 min RT with high recovery of 94.2%–99.5% and an average binding capacity of 83.8 mg/mL (Fan et al., 2021). The AEX-TEA membrane exhibited a high binding capacity for pure AAV2 of 9.6×10^{13} capsids/mL at 1.0 min residence time and outperformed Sartobind Q membranes by isolating AAV2 from a Sf9 lysate with high productivity of 2.4×10^{13} capsids·mL $^{-1}$ ·min $^{-1}$ and HCPs removal of nearly 1.8 LRV (Fan et al., 2022). The CEX-IDA and AEX-TEA membranes used in series to purify the AAV2 from the Sf9 lysate achieved a total capsid recovery of 65.3% with an infective recovery of 76%, higher than those reported using ion-exchange resin chromatography (Fan et al., 2022).

5 | STAPLE FIBROUS SYSTEMS

Winderl et al. (2018) studied the flow behavior and binding characteristics winged-shaped fibers of PA6 with effective fiber diameters of 15–20 μm , as shown in Figure 4. These fibers had a reported intrinsic surface area of 2 m 2 /g and fiber length of approximately 6 mm. The fiber surfaces were modified by free a

layer of GMA via free radical polymerization, at three different grafting densities. The epoxy groups were then reacted with sodium sulfate to form strong cation exchange membranes. Rather than forming a web, the fibers were suspended in a packing solution of 1 g of fiber per 500 mL of solution, introduced into a 0.66 cm diameter column that was drained and adjusted to the desired column height (1–4 cm) with adjustable endpieces. In essence, this is an example of a wetlay process, as described above, where the fibers are being deposited directly into the separation device. This is a technique that is scalable and could be used with a variety of different columns and membrane formats. Careful hydrodynamic studies were performed, and the equilibrium and dynamic binding capacities of the fibers for lysozyme were measured. Experiments were also done to measure the chromatographic resolution of the packed columns using a three-component model protein mixture of lysozyme, cytochrome c and a mAb. The results were compared with the performance of commercial chromatographic resins. The equilibrium binding capacities reported were in the range of 10–35 mg lys/mL of column, while dynamic binding capacities were in the range of 5–15 mg lys/mL of column. There was an observed drop in dynamic binding capacity with increasing flow rate (reduced residence time), indicating some diffusional resistance to protein adsorption within the hydrogel grafted layer, in agreement with the observations of other researchers working with similarly grafted fibrous systems.

In an earlier study, Schwellenbach et al. (2016) used winged fibers from the same source and with very similar shape as those described in the work of Winderl et al. (2018) but made out of PET. They reported an effective diameter of approximately 15 μm and the same intrinsic surface area of 2 m²/g. These fibers were first aminated and then grafted with a hydrogel layer of pGMA using SI-ATRP. Sodium sulfite was used to create a strong cation exchange functionality. As opposed to the work of Winderl et al. (2018) the fibers were first suspended in an ethanol solution to remove aggregates and then dried. The dried fibers were packed in a 1 cm column and packed to a bed height of 3 cm. Since the fibers were dry, this approach comes close to what could be done by using the airlay processing as described previously. There are technologies to scale up this approach to generate packings for flat sheets or columns that could be used to deploy this approach in a larger effort. Protein equilibrium and dynamic capacity measurements were carried out for both lysozyme and IgG and compared to the performance of a strong cation exchange Fractogel[®] chromatographic resin and Sartobind[®] S, a strong cation exchange cast membrane. A mixture of four proteins, including lysozyme, BSA, a mAb, and myoglobin was studied in separation experiments. The equilibrium binding capacities for lysozyme and hIgG were 90 and 92 mg/mL, respectively, while the dynamic binding capacities were 50 and 54 mg/mL. Dynamic binding capacities (DBC) were measured with residence times (RT) in the range of 10–60 s. A slight decrease in DBC with decreasing RT was observed for the winged fibers, but significant drops in DBC were found for both the Fractogel[®] and the Sartorius[®] S membrane. The winged fiber static binding capacities were larger than those for the cast membranes but were significantly lower than those for the

chromatographic resin. The flow permeability of the fibrous column at high ionic strength was 10 times larger than that of the cast membrane (500 mDa vs. 50 mDa). In agreement with work done by other investigators, the authors attributed the high binding capacity at low ionic strength to the expansion of the hydrogel due to charge repulsion in low conductivity solutions. Using a salt gradient, it was possible to effectively separate the four proteins in the sample mixture with good resolution.

Winderl et al. (2021) used the two types of strong cation exchanged winged fibers as prepared by Winderl et al. (2018) and Schwellenbach et al. (2016) in a study to examine the ability of these fibrous systems to remove antibody aggregates from cell culture supernatants in both a frontal and bind-and-elute mode. In the bind-and-elute model, the aggregates are removed during the elution step, while in frontal chromatography the column is loaded beyond breakthrough under conditions favoring aggregate binding and an aggregate-depleted pool is collected during the loading step. The sample used was a mAb in a CHO cell culture supernatant purified by Protein A chromatography containing 4.87% dimers and 1.16% trimers. In this case, both strong cation exchange winged fibers: (1) PA6 with GMA grafting by free radical polymerization (FRP) and (2) PET fibers with GMA grafted by SI-ATRP, were packed dry into a 0.66 cm and 0.88 cm diameter columns using the Schwellenbach et al. technique. Because of their large fiber diameter, the relative permeabilities of the fibrous systems were much larger than those cast membranes. The SI-ATRP fibers outperformed the FRP fibers, and exhibited DBCs for mAb of 41–20 mg/mL over the range of RT from 0.2 to 1.5 min. The SI-ATRP fibrous system also outperformed the POROS HS resin commonly used for aggregate removal, especially at the shorter residence times. The authors also estimated that although the buffer use of the fibrous materials is higher, the productivity of the POROS HS is smaller.

6 | ELECTROSPUN NONWOVENS

Most of the academic work on fibrous membranes for bioseparations relies on web formation by electrospinning, primarily due to its ability to form sub-micron fibers. Thanks to the flexibility of electrospinning, membrane mats are produced using various polymers that can be modified to add different functionalities. Ethylene-vinyl alcohol (EVAL), cellulose, cellulose acetate, nylon, copolymers and silk nanofibers have been functionalized as anion and cation exchangers, with multimodal ligands as well as with metal chelate groups (Amaly, El-Moghazy, et al., 2018, 2020, 2020; Cheng et al., 2022; Duan et al., 2018; Fu et al., 2016, 2019; Wang et al., 2019) while Shan et al. has produced inorganic nanofibrous membranes (Fu et al., 2022; Shan et al., 2017). All materials have been characterized in terms of structural and surface properties and tested for adsorption mainly with pure protein solutions in batch adsorption experiments obtaining static binding capacities for lysozyme as high as 716 mg/g for the BTCA@EVAL-3 membrane (Fu et al., 2019) and of 10 mg/g of the silk nanofibers

functionalized with carboxylic groups (Yi et al., 2017) that were among the best performing materials. Breakthrough experiments were limited to pure protein solutions, mostly under gravity as driving force. The dynamic binding capacity obtained was nearly 70% of the SBC, however, the DBC at 10% breakthrough was only 261 mg/g (Fu et al., 2019), indicating the presence of dispersive effects that are most likely due to mass transfer limitations. Water or buffer flux data were rarely available, and permeability studies were performed only at very low-pressure drops, but the limited results show a promising permeability. Moreover, no tests have been performed with cell culture supernatants or real fluids from the biopharmaceutical industry. In fact, to determine the real applicability of these materials in industrial applications, tests at higher flow rates should be performed and real cell culture fluids must be used as feed solutions.

The AEX-TEA membrane exhibited a high binding capacity for pure AAV2 of 9.6×10^{13} capsids/mL at 1.0 min residence time and outperformed Sartobind Q membranes by isolating AAV2 from an Sf9 lysate with high productivity of 2.4×10^{13} capsids·mL⁻¹·min⁻¹ and HCPs removal of nearly 1.8 LRV (Todd Menkhaus, Hao Fong and colleagues at the South Dakota School of Mines (Rapid City, SD, USA) demonstrated the production of electrospun mats of cellulose acetate nanofibers, with fiber distributions from tens of nanometers to the micron scale. In this case, the large fibers provide structural and mechanical integrity, while the small fibers provide high surface areas for adsorption. These structures were functionalized with DEAE for anion-exchange functionality. The result was a maximum theoretical dynamic binding capacity of 33.3 mg BSA/g, while permeability of the electrospun membrane compared to commercial regenerated cellulose was found to be 4-6 times higher throughout the range of multilayer constructions tested (L. Zhang et al., 2008). Later work built upon this core structure, with the addition of three-dimensional grafted adsorption layers via ATRP of poly(acrylic acid) (PAA) onto the cellulose acetate nanofibers. This work demonstrated a 50-fold increase in protein binding capacity compared to a traditional micron-scale membrane-based device and validated that the surface layers providing improved capacity did not significantly reduce the kinetics of adsorption. The permeability of these structures was found to be more than an order of magnitude higher than an agarose resin packed bed column, though the PAA coating was found to swell and therefore decrease the membrane permeability under lower conductivity buffer conditions (Menkhaus et al., 2010). Their technology was brought to market by Nanopareil, a company that was subsequently acquired by Astrea Bioseparations, and commercialized as AstreAdept laboratory filtration devices. These products will be discussed in the section that follows.

In more recent work from the same group, cellulose graft-polypropionic acid (CL-g-PPA) cation-exchange nanofiber membranes were prepared and characterized in view of their possible application for the separation of biomolecules (Rajesh et al., 2017). The same base nanofiber mats were used to graft polyethylenemidoamine, obtaining CL-g-PEAA anion-exchange nanofiber membranes (Rajesh et al., 2018). The CEX membranes had lysozyme

SBC of 1664 mg/g and a DBC_{10%} of 206 mg/mL, while the AEX adsorbers showed a BSA SBC of 239 mg/g and a DBC_{10%} of 31 mg/mL. Moreover, the AEX membranes were also challenged for filtration of polystyrene particles on the nanometer range (40–200 nm diameter) as to demonstrate their potential application to bind protein and separate larger particles such as cells, cell debris or viruses by size exclusion. However, the membranes were not tested in competitive conditions with mixtures, nor with real biological fluids, therefore their behavior and their propensity to fouling is unknown (Rajesh et al., 2018).

7 | NONWOVEN COMMERCIAL MEMBRANES FOR DOWNSTREAM PROCESSING

The field of commercial membrane adsorbers is dominated by products made with microporous membranes as a support for ligand attachment, however, new products based on fibrous materials have been developed in recent years. While Astrea Bioseparations focuses more in laboratory scale batch spin filters, MilliporeSigma (Natrix[®] membranes) and Cytiva (Fibro[™] chromatography) produce membrane adsorbers targeted at industrial scale separation of biologics that can be used for capture and polishing steps. Other products based on fibrous filters, manufactured by 3M, are proposed for clarification and impurity removal before chromatographic steps. All these commercial units are based on flat sheet membrane materials. They are arranged in layers or as a single fibrous bed made by compressing several layers.

7.1 | Fibrous materials for clarification and impurity removal

3M Emphaze[™] AEX Hybrid Purifier is chromatographic hybrid clarification filter that incorporates four layers of functionalized polypropylene nonwoven with grafted positively charged quaternary ammonium followed by a 0.2 μm microporous polyamide membrane (Van de Velde et al., 2020). The filtration device can be used to remove DNA, HCPs, chromatin heteroaggregates, and associated impurities from cell cultures in dead-end filtration mode during clarification for mAb production, and is usually follows a conventional depth filter (Almeida et al., 2022; Castro-Forero et al., 2015; Metzger et al., 2020). The early reduction of impurities by this chromatographic filter lightens the workload in subsequent unit operations and simplifies the overall purification process (Castro-Forero et al., 2015; Metzger et al., 2020). Van de Velde et al. (2020) found that the effective removal of DNA and chromatin before the protein A column reduced the co-eluted HCPs by a factor of 10, compared to the case without chromatographic clarification. Koehler reported a DNA reduction of nearly 5-log after clarification by Emphaze[™] AEX Hybrid Purifier at a throughput of 200 L/m², with a 24-fold improvement in HCP removal after protein A chromatography (Koehler et al., 2019).

This would allow for shorter, less aggressive, and less frequent regeneration and sanitization for protein A column (Koehler et al., 2019), due to which the productivity of a protein A periodic counter-current chromatography (PCC) with four columns can be improved by 49% over 100 cycles, as reported by El-Sabbahy et al. (2018). Gilgunn et al. (2019) found that chromatographic filter inclusion was also effective in removing some problematic HCPs. Metzger et al. (2020) studied the performance for clarification of an *Escherichia coli* homogenate and found that it not only improved the removal of DNA, HCPs, and endotoxins in the homogenate, but also better preserved the binding capacity for the expressed fibroblast growth factor 2 in the subsequent cation exchange chromatography.

The process performance could be further improved with a new stand-alone filter device, 3M™ Harvest RC, for chromatographic clarification of a variety of cell cultures to capture whole cells, cell debris, and soluble impurities in a single step. This filter eliminates the need for depth filtration that decreased the overall product cost with less operational complexity, higher loading capacity, product recovery, and impurity removal (Almeida et al., 2022).

Following the same principle of combining different layers with different functionalities into one filter so as to reduce process stages is the AEX disposable Polisher ST capsule (3M™ Polisher ST). The hybrid unit comprises functional Q nonwovens and salt-tolerant guanidinium functional membranes (Hester et al., 2020). The guanidinium ligand provided robust clearance of HCPs and viruses in a variety of buffers over a wide range of pH and conductivities up to 20 mS/cm (Hester et al., 2020). The 3M™ Polisher ST has been shown to be suitable for the treatment of turbid fluids after low-pH viral inactivation following protein A chromatography in mAb purification, as it can truly replace the depth filtration and anion exchange column chromatography used in the traditional purification process (Hester et al., 2020; Singh et al., 2017). By combining Emphaze™ AEX Hybrid Purifier for clarification before protein A chromatography, Singh et al. (2017) realized a two-step process for mAb purification which reduced one chromatographic step in the traditional purification train. All 3M filter types described above are available in small-scale unit for process development studies and as modular scale-up units for manufacturing.

7.2 | Fibrous materials for membrane chromatographic operations

As mentioned previously, Astrea Bioseparations recently purchased Nanopareil, and has commercialized a product based on composite nanofiber structures that comprise both cellulosic and noncellulosic materials in a multi-layer bicomponent structure: the result is material with increased strength due to larger, approximately 575 nm average fiber diameter cellulose nanofibers, and high-capacity functional synthetic fibers with 200 nm average diameter. The result of these developments is a membrane capable of high flowrate operation as one would expect from a nonwoven-based separation device, and an elevated dynamic binding capacity of 120 mg/mL for BSA when

functionalized as a weak ion-exchanger (Ahmad, 2022). Currently, this technology has been implemented into a spin filter format for viral vector purification at the lab scale, in the Nereus LentiHERO product, which was able to purify lentiviral vectors (LV) from an HEK293 feedstock with recovery yield higher than 60% and a 95% reduction in HCP contaminants in a simple benchtop centrifuge format, without ultracentrifugation or chromatography. This enables rapid concentration viral vector feedstocks, offering a new laboratory-scale alternative to traditional ion-exchange chromatography and ultrafiltration steps (Steel, 2022).

Natrix and Fibro™ chromatographic membranes originated from academic groups and small spin-off companies that developed the technology, Natrix Separations and Puridify. These membranes can operate at short residence times with high binding capacities and target the same market, but their membrane structures are different. Natrix membranes consist of flat sheet functionalized macroporous hydrogels coated on polyolefin nonwoven supports (Hassel & Moresoli, 2016; Hou et al., 2015) that are available on different formats, from small 0.2 mL units to 460 mL modules. The interconnected pore structure was reported to offer high surface area for protein binding and allowed operation at high flow rates due to the convective mass transport (Hou et al., 2015). Hassel and Moresoli (2016) observed that the pore size of a weak cation exchange (Natrix® C) hydrogel membranes varies from 0 to 1.6 μm and found that solution pH and ionic strength have a great impact on the pore size, as the charge of the ligand changes, causing the associated repulsion, water uptake and membrane swelling to change. The DBC_{10%} for polyclonal IgG of this membrane is estimated to be nearly 100 mg/mL at 1–5 mL/min (0.08–0.4 min RT) (Hassel & Moresoli, 2016; Hou et al., 2015) observed a DBC_{10%} of 74 mg/mL at 0.1 min RT for capturing a mAb from a clarified culture fluid and the Natrix® C membrane had good reproducibility in yield and product purities for more than 30 cycles, which is helpful for improving manufacturing flexibility and productivity. In addition, the anion exchange (Natrix® Q) membranes for mAb polishing in flowthrough mode exhibited a significantly higher binding capacity for impurities which supported mAb loads up to 10 kg/L, and 40 times faster processing speed compared to traditional AEX column chromatography (Hou et al., 2015).

Pollard et al. (2016) proposed a two-step process based on Natrix disposable adsorbers for mAb purification: they used a prototype protein A membrane for mAb capture and the Natrix® Q membrane for subsequent polishing. Both capture and polishing steps were significantly faster (30–60 times) than homologous resins. The high-throughput process had three-fold higher productivity, provided favorable impurity removal, and is estimated to have reduced costs by nearly 40% (Pollard et al., 2016). Pereira Aguilar et al. (2020) applied (Natrix® Q) membrane to capture enveloped virus-like particles (eVLPs) directly from cell culture supernatant. The membrane achieved the highest binding capacity for viral particles with a much shorter residence time than Q monolith and resins particles, due to its larger accessible surface area for binding large molecules and convective flow property. However, it was unable to

separate eVLPs from host cell-derived particles (Pereira Aguilar et al., 2020).

Electrospun nanofiber mats from regenerated cellulose with average fiber diameters on the scale of 500 nm are the base materials for Cytiva's Fibro™ line of products that provides units of 0.4 and 3.75 mL membrane volume. Their manufacturing principle was demonstrated by Dods et al. (2015), where they were able to obtain a cellulose fiber mat of 30 g/m² and compressed up to 12 layers together with a heat press. Figure 1 shows a photo of the sub-micron fibers produced by electrospinning in this application. The cellulose fiber mat was functionalized with DEAE for anion exchange functionality to bind BSA and oxidized via TEMPO (2,2,6,6-tetramethylpiperidine 1-oxyl) oxidation for cation exchange capture of lysozyme. The pressure drops reported were largely below 2 bar, though experiments with large numbers of layers compressed at high pressure reached 4 or more bar, especially as flow rates were raised above 300 cm/h up to 600 cm/h. Most importantly, static binding capacities up to 27.4 mg BSA/mL and 47.5 mg lysozyme/mL were demonstrated for anion and cation exchange, respectively. In flow studies, dynamic binding capacities reached 12 mg BSA/mL, 21 mg lysozyme/mL and were largely independent of flow rate within the range tested (Dods et al., 2015). The authors did demonstrate that more highly compressed membranes experienced decreased capacity, likely due to the closing of pores and resulting reduction of available surface area.

More recently, Fibro™ membranes were tested for purification of biologics, Zhang et al. (2021) compared side by side a Mabselect Prisma resin with Fibro™ Prisma membrane for the separation of single-arm species from IgG-like bispecific antibody products. It is important to note that for the same ligand, the resin showed low impurity removal capacity, limiting the mass fraction of the eluate containing the byproduct to 15.9%. In contrast, due to the rapid mass transfer achieved in the Fibro™ application, it was possible to demonstrate complete removal of the single-arm byproduct and achieve a product yield of 80.2% (T. Zhang et al., 2021). In another application, Fibro™ Prisma adsorbers were used to capture a tetravalent bispecific antibody from a low titer clarified HEK293 fed-batch cell culture at a residence time of 7.5 s. The affinity purification required 4.5 h as compared to 1–2 days that would be needed to process the 8 L batch with a resin column without compromising yield and purity (Napoleone et al., 2021).

The higher flow rates enabled by convective mass transfer and low-pressure drops allow extremely high cycle rates in bind-elute configurations. This can be advantageous in any manufacturing environment, but it is viewed as particularly favorable in the burgeoning field of gene therapies, where product titers are significantly lower than in traditional mAb manufacturing processes. Ruscic et al. (2019) used the Fibro™ system with Q functionalization to demonstrate up to 90% recovery of biologically active lentiviral vectors from HEK293 cell culture media and achieved a 2-log removal of HCPs. In addition, they found that the typical TFF concentration step required before resin chromatography caused a loss of product, which was made obsolete by using the Fibro™

chromatography media, which did not require concentration to achieve reasonable processing times.

Similarly, Turnbull et al. (2019) demonstrated the use of the same system to capture adenovirus 5 viral vectors from HEK293 media. They studied the impact of variation in ligand density and binding duration on product infectivity and yields. Most critically, it has been shown that 100% recovery can be achieved at low retention times, though high ligand densities have been found to negatively impact capsid infectivity. Because the yields of many viral vector production systems are very low, the limited capacity of nonwovens compared to resins is not a significant negative factor, and the 29-fold increase in productivity over resin systems would result in significant cost savings.

8 | DISCUSSION AND CONCLUSIONS

Romero et al. (2023) developed a thorough computational framework to evaluate the performance of antibody capture processes and considered the use of Prisma resin chromatography column, a Purexa™ PrA cast membrane, and a Fibro™ Prisma nonwoven fabric membrane. The results showed that in single-cycle operations the cost of goods of the resin approach was 28%–30% lower than those of either membrane. However, the process time for using columns was estimated to be 107 and 122 times higher than the Fibro™ Prisma and the Purexa™ PrA membranes, respectively. The shorter process times are key for the success of disposable platforms, and the disposable equipment also reduces process footprints, eliminates sanitization and cleaning steps, cuts down on the process footprint. These studies were done at the milliliter scale, and the authors pointed out that none of the membrane manufacturers currently offer membranes for product capture that can be used in large-scale processes.

Nonwoven fabrics have great potential for ultimately being used in a process scale, even for product capture steps, and to enable truly novel approaches to the purification of biologics. For example, 3 M membrane product lines for the clarification of cell culture supernatants and the removal of HCPs, and other impurities are based on nonwoven fabrics and are available for use at larger scales. They also enable alternative process capabilities that may reduce process steps and processing time.

In this vein, the benefits offered by membrane chromatographic devices have begun to be demonstrated in studies investigating potential process improvements such as continuous downstream processing approaches. The potential for increased productivity was studied by Hardick et al. (2015) in a simulated moving bed system using DEAE functionality to separate BSA from cytochrome C. The study demonstrates a 10-min simulated moving bed (SMB) run, with a 7 s bind-elute cycle per column. The resulting productivity of the system was found to be 3.92 g/mL/h, more than an order of magnitude improvement over porous resin column systems. The authors also state that, if not for the mechanical limitation of the pumps used in the study, the productivity of the fiber-based

approach would reach 26 g/mL/h (Hardick et al., 2015). More recently, Davis et al. (2021) compared periodic countercurrent chromatography (PCC) utilizing Fibro™ HiTrap PrismA and MabSelect PrismA resin columns. Under manufacturer-recommended conditions, the productivity for the perfusion system with titers of 0.2 g/L and 1 g/L titers were 45 and 12 times higher than the comparable resin-based system. Most importantly, their cost analysis of the process found that downstream processing costs could be reduced by up to 90% using fiber chromatography systems, largely due to the decreases in labor and time costs associated with decreased operating time for a given unit operation (Davis et al., 2021). These factors, in conjunction with the growing body of knowledge surrounding the economic benefits of single-use technologies, make a compelling case for the adoption of membrane-based devices (Lopes, 2015).

Moreover, these benefits are not limited to a single pharmaceutical modality or manufacturing paradigm. The work presented here indicates that there are numerous ways of modifying the surface properties of nonwoven fabrics to serve almost any application. The nonwoven membranes have clear advantages in terms of large pore size to be able to adsorb large biologics such as viral vector and large proteins, and they largely eliminate diffusional limitations during product binding and elution. In addition, many groups have already been able to develop nonwoven membranes that have binding capacities per unit volume of membrane that are the same, or sometimes even higher, than the binding capacity of ion exchange and Protein A affinity resins, and at shorter residence times. However, many groups accomplished this by using sub-micron fiber diameters generated by electrospinning to increase the surface area of the membrane and the binding capacity. As shown in this paper, this approach greatly decreases the flow permeability, and reduces the thickness of the membrane that can be used at short residence times and at pressures that are compatible with biopharmaceutical processes. Other groups have used larger fibers that reduce pressure drop, but to increase the binding capacity they require thicker grafted layers of various hydrogels to enable binding capacities much greater than can be achieved through monolayer protein binding on the fiber surface. Finally, some investigators have focused on the use of larger fiber diameters of lobed, or winged fibers with increased surface areas that go one step further in enhancing binding capacities with lower pressure drops.

Ultimately, progress in the area of nonwoven membrane fabrication using bi-component systems that include large supporting fibers together with large surface area additives or surface treatments is likely to succeed in reaching the goal of high DBC, short residence times, and low pressure drops required to eliminate resin packed columns for product capture in downstream separations.

AUTHOR CONTRIBUTIONS

Joseph Lavoie: Conceptualization; writing—original draft; writing—review & editing. **Jinxin Fan:** Conceptualization; writing—original draft; writing—review & editing. **Behnam Pourdeyhimi:** Conceptualization;

writing—original draft; writing—review & editing. **Cristiana Boi:** Conceptualization; supervision; writing—original draft; writing—review & editing. **Ruben G. Carbonell:** Conceptualization; supervision; writing—original draft; writing—review & editing; funding acquisition.

ACKNOWLEDGMENTS

This work was funded by the Novo Nordisk Foundation (Grant #NNF19SA0035474), as part of the Accelerating Innovation in the Manufacturing Biologics (AIM-Bio) program, and by the William R. Kenan, Jr. Institute for Engineering, Technology & Science at North Carolina State University.

DATA AVAILABILITY STATEMENT

Data sharing is not applicable to this article as no datasets were generated or analyzed during the current study.

ORCID

Cristiana Boi  <http://orcid.org/0000-0002-7264-9496>

REFERENCES

- Ahmad, B. (2022). A radical change in bioprocessing for cell and gene therapies. *Bioprocess International*, 20 (Nov–Dec).
- Almeida, A., Chau, D., Coolidge, T., El-Sabbahy, H., Hager, S., Jose, K., Nakamura, M., & Voloshin, A. (2022). Chromatographic capture of cells to achieve single stage clarification in recombinant protein purification. *Biotechnology Progress*, 38(2), e3227. <https://doi.org/10.1002/btpr.3227>
- Amaly, N., El-Moghazy, A. Y., Si, Y., & Sun, G. (2020). Functionalized nanofibrous nylon 6 membranes for efficient reusable and selective separation of laccase enzyme. *Colloids and Surfaces B: Biointerfaces*, 194, 111190. <https://doi.org/10.1016/j.colsurfb.2020.111190>
- Amaly, N., Ma, Y., El-Moghazy, A. Y., & Sun, G. (2020). Copper complex formed with pyridine rings grafted on cellulose nanofibrous membranes for highly efficient lysozyme adsorption. *Separation and Purification Technology*, 250, 117086. <https://doi.org/10.1016/j.seppur.2020.117086>
- Amaly, N., Si, Y., Chen, Y., El-Moghazy, A. Y., Zhao, C., Zhang, R., & Sun, G. (2018). Reusable anionic sulfonate functionalized nanofibrous membranes for cellulase enzyme adsorption and separation. *Colloids and Surfaces B: Biointerfaces*, 170, 588–595. <https://doi.org/10.1016/j.colsurfb.2018.06.019>
- Batra, S. K., & Pourdeyhimi, B. (2012). *Introduction to nonwovens technology*. DEStech Publications, Inc.
- Bird, R. B., Stewart, W. E., & Lightfoot, E. N. (2001). *Transport phenomena* (2nd ed.). Wiley.
- Boi, C. (2018). Membrane chromatography for biomolecule purification. In A. Basile & C. Charcosset, (Eds.), *Current trends and future developments on (bio-) membranes: Membrane processes in the pharmaceutical and biotechnological field* (pp. 151–166). Elsevier. <https://doi.org/10.1016/C2016-0-04295-X>
- Castro-Forero, A. A., Jokondo, Z., Voloshin, A., & Hester, J. F. (2015). Anion-exchange chromatographic clarification: Bringing simplification, robustness, and savings to MAb purification. *Bioprocess International* (June).
- Chappas, W., & Pourdeyhimi, B. (2013). *Composite filter media with high surface area fibers* (Patent No. 8,410,006). U.S. Patent and Trademark Office.
- Chen, S.-T., Wickramasinghe, S. R., & Qian, X. (2020). Electrospun Weak Anion-Exchange Fibrous Membranes for Protein Purification. *Membranes*, 10(3), 39. <https://doi.org/10.3390/membranes10030039>

- Cheng, P., Ji, C., Hu, W., Huang, P., Guo, Q., Xia, M., Cheng, Q., Xu, J., Liu, K., & Wang, D. (2022). Facile fabrication of nanofibrous ion-exchange chromatography membrane with aminated surface for highly efficient RNA separation and purification. *Colloids and Surfaces, A: Physicochemical and Engineering Aspects*, 648, 129160. <https://doi.org/10.1016/j.colsurfa.2022.129160>
- Davies, C. N. (1953). The separation of airborne dust and particles. *Proceedings of the Institution of Mechanical Engineers, Part B: Management and Engineering Manufacture*, 1(1-12), 185-213. <https://doi.org/10.1177/095440545300100113>
- Davis, R. R., Suber, F., Heller, I., Yang, B., & Martinez, J. (2021). Improving mAb capture productivity on batch and continuous downstream processing using nanofiber Prisma adsorbents. *Journal of Biotechnology*, 336, 50-55. <https://doi.org/10.1016/j.jbiotec.2021.06.004>
- Dods, S. R., Hardick, O., Stevens, B., & Bracewell, D. G. (2015). Fabricating electrospun cellulose nanofibre adsorbents for ion-exchange chromatography. *Journal of Chromatography A*, 1376, 74-83. <https://doi.org/10.1016/j.chroma.2014.12.010>
- Duan, C., Fu, Q., Si, Y., Liu, L., Yin, X., Ji, F., Yu, J., & Ding, B. (2018). Electrospun regenerated cellulose nanofiber based metal-chelating affinity membranes for protein adsorption. *Composites Communications*, 10, 168-174. <https://doi.org/10.1016/j.coco.2018.09.010>
- El-Sabbahy, H., Ward, D., Ogonah, O., Deakin, L., Jellum, G. M., & Bracewell, D. G. (2018). The effect of feed quality due to clarification strategy on the design and performance of protein A periodic counter-current chromatography. *Biotechnology Progress*, 34(6), 1380-1392. <https://doi.org/10.1002/btpr.2709>
- Erickson, J., Baker, J., Barrett, S., Brady, C., Brower, M., Carbonell, R., Charlebois, T., Coffman, J., Connell-Crowley, L., Coolbaugh, M., Fallon, E., Garr, E., Gillespie, C., Hart, R., Haug, A., Nyberg, G., Phillips, M., Pollard, D., Qadan, M., ... Lee, K. (2021). End-to-end collaboration to transform biopharmaceutical development and manufacturing. *Biotechnology and Bioengineering*, 118(9), 3302-3312. <https://doi.org/10.1002/bit.27688>
- Etzel, M. R. (2003). Chapter 10 layered stacks. In F. Švec, T. B. Tennikova & Z. Deyl, (Eds.), *Journal of Chromatography Library* (67, 1st ed., pp. 213-234). Elsevier. [https://doi.org/10.1016/S0301-4770\(03\)80026-X](https://doi.org/10.1016/S0301-4770(03)80026-X)
- Fan, J., Barbieri, E., Shastry, S., Menegatti, S., Boi, C., & Carbonell, R. G. (2022). Purification of adeno-associated virus (AAV) serotype 2 from *Spodoptera frugiperda* (Sf9) lysate by chromatographic nonwoven membranes. *Membranes*, 12(10), 944. <https://doi.org/10.3390/membranes12100944>
- Fan, J., Boi, C., Lemma, S. M., Lavoie, J., & Carbonell, R. G. (2021). Iminodiacetic acid (IDA) cation-exchange nonwoven membranes for efficient capture of antibodies and antibody fragments. *Membranes*, 11(7), 530. <https://doi.org/10.3390/membranes11070530>
- Fan, J., Luo, J., Song, W., Chen, X., & Wan, Y. (2015). Directing membrane chromatography to manufacture α 1-antitrypsin from human plasma fraction IV. *Journal of Chromatography A*, 1423, 63-70. <https://doi.org/10.1016/j.chroma.2015.10.050>
- Fan, J., Sripada, S. A., Pham, D. N., Linova, M. Y., Woodley, J. M., Menegatti, S., Boi, C., & Carbonell, R. G. (2023). Purification of a monoclonal antibody using a novel high-capacity multimodal cation exchange nonwoven membrane. *Separation and Purification Technology*, 317, 123920. <https://doi.org/10.1016/J.SEPPUR.2023.123920>
- Fu, Q., Si, Y., Liu, L., Yu, J., & Ding, B. (2019). Elaborate design of ethylene vinyl alcohol (EVAL) nanofiber-based chromatographic media for highly efficient adsorption and extraction of proteins. *Journal of Colloid and Interface Science*, 555, 11-21. <https://doi.org/10.1016/j.jcis.2019.07.065>
- Fu, Q., Wang, X., Si, Y., Liu, L., Yu, J., & Ding, B. (2016). Scalable fabrication of electrospun nanofibrous membranes functionalized with citric acid for high-performance protein adsorption. *ACS Applied Materials & Interfaces*, 8(18), 11819-11829. <https://doi.org/10.1021/acsami.6b03107>
- Fu, Q., Xie, D., Ge, J., Zhang, W., & Shan, H. (2022). Negatively charged composite nanofibrous hydrogel membranes for high-performance protein adsorption. *Nanomaterials*, 12(19), 3500. <https://doi.org/10.3390/nano12193500>
- Galiano, F. (2020). Immersion casting. In E. Driolo & L. Giorno, (Eds.), *Encyclopedia of membranes* (pp. 1-2). Springer. <https://doi.org/10.1007/978-3-642-40872-4>
- Gilgunn, S., El-Sabbahy, H., Albrecht, S., Gaikwad, M., Corrigan, K., Deakin, L., Jellum, G., & Bones, J. (2019). Identification and tracking of problematic host cell proteins removed by a synthetic, highly functionalized nonwoven media in downstream bioprocessing of monoclonal antibodies. *Journal of Chromatography A*, 1595, 28-38. <https://doi.org/10.1016/j.chroma.2019.02.056>
- Goeminne, H., de Bruyne, R., & Roos, J. (1974). Geometrical and filtration characteristics of metal-fibre filters: A comparative study. *Filtration & Separation*, 11(4), 351-355.
- Gurgel, P. V., Zheng, Y., Burton, S. J., & Carbonell, R. G. (2012). *High-surface area fibers and nonwoven membranes for use in bioseparations* (Patent No. 2012/068442). World Intellectual Property Organization.
- Hardick, O., Dods, S., Stevens, B., & Bracewell, D. G. (2015). Nanofiber adsorbents for high productivity continuous downstream processing. *Journal of Biotechnology*, 213, 74-82. <https://doi.org/10.1016/j.jbiotec.2015.01.031>
- Hassel, K. J., & Moresoli, C. (2016). Role of pH and ionic strength on weak cation exchange macroporous hydrogel membranes and IgG capture. *Journal of Membrane Science*, 498, 158-166. <https://doi.org/10.1016/j.memsci.2015.08.058>
- Heller, M., Carbonell, R. G., & Pourdeyhimi, B. (2021). *Grafted islands-in-the-sea nonwoven for high capacity ion exchange separations* (Patent No. 11,027,243). U.S. Patent and Trademark Office.
- Heller, M. L. (2015). Polymer grafted nonwoven membranes for bioseparations. North Carolina State University.
- Heller, M., Li, Q., Esinhart, K., Pourdeyhimi, B., Boi, C., & Carbonell, R. G. (2020). Heat induced grafting of Poly(glycidyl methacrylate) on polybutylene terephthalate nonwovens for bioseparations. *Industrial & Engineering Chemistry Research*, 59(12), 5371-5380. <https://doi.org/10.1021/acs.iecr.9b04936>
- Heller, M., Wimbish, R., Gurgel, P. V., Pourdeyhimi, B., & Carbonell, R. G. (2016). Reducing diffusion limitations in ion exchange grafted membranes using high surface area nonwovens. *Journal of Membrane Science*, 514, 53-64. <https://doi.org/10.1016/j.memsci.2016.02.046>
- Hester, J., Heitkamp, J., Peters, M., Jokondo, Z., & Rasmussen, J. (2020). Streamlined polishing and viral clearance. *Bioprocess Online*, 18(10), 1-9.
- Hou, Y., Brower, M., Pollard, D., Kanani, D., Jacquemart, R., Kachuik, B., & Stout, J. (2015). Advective hydrogel membrane chromatography for monoclonal antibody purification in bioprocessing. *Biotechnology Progress*, 31(4), 974-982. <https://doi.org/10.1002/btpr.2113>
- Jian, S.-J., Wang, S. S.-S., Ooi, C. W., Hoe, B. C., Lai, Y.-R., Chiu, C.-Y., Hsu, M., Chen, K.-H., & Chang, Y.-K. (2022). Cellulose-based nanofiber membrane functionalized with dye affinity ligand for purification of malate dehydrogenase from *Saccharomyces cerevisiae*. *Cellulose*, 29(17), 9251-9281. <https://doi.org/10.1007/s10570-022-04815-z>
- Kim, Y., Rana, D., Matsuura, T., Chung, W. J., & Khulbe, K. C. (2010). Relationship between surface structure and separation performance of poly(ether sulfone) ultra-filtration membranes blended with surface modifying macromolecules. *Separation and Purification*

- Technology, 72(2), 123–132. <https://doi.org/10.1016/j.seppur.2010.01.006>
- Klein, E. (1991). *Affinity membranes: Their chemistry and performance in adsorptive separation processes*. Wiley. <https://www.wiley.com/en-us/Affinity%2BMembranes%3A%2BTheir%2BChemistry%2Band%2BPerformance%2Bin%2BAbsorptive%2BSeparation%2BProcesses-p-9780471527657>
- Koehler, K. C., Jokondo, Z., Narayan, J., Voloshin, A. M., & Castro-Forero, A. A. (2019). Enhancing protein A performance in mAb processing: A method to reduce and rapidly evaluate host cell DNA levels during primary clarification. *Biotechnology Progress*, 35(6), e2882. <https://doi.org/10.1002/btpr.2882>
- Lemma, S. M., Boi, C., & Carbonell, R. G. (2021). Nonwoven ion-exchange membranes with high protein binding capacity for bioseparations. *Membranes*, 11(3), 181. <https://doi.org/10.3390/membranes11030181>
- Liu, H. C., & Fried, J. R. (1994). Breakthrough of lysozyme through an affinity membrane of cellulose-cibacron blue. *AIChE Journal*, 40(1), 40–49. <https://doi.org/10.1002/AIC.690400107>
- Liu, H., Gurgel, P. V., & Carbonell, R. G. (2015). Preparation and characterization of anion exchange adsorptive nonwoven membranes with high protein binding capacity. *Journal of Membrane Science*, 493, 349–359. <https://doi.org/10.1016/j.memsci.2015.06.002>
- Liu, W., Chiang, D., Chen, J., & Susuki, R. (2005). Electrostatic investigation of charged nanoporous electret materials. *ISE-12: 12th International Symposium on Electrets: Proceedings: 11–14 September 2005, Salvador, Bahia, Brazil*, (pp. 35–38).
- Long, Y.-Z., Yan, X., Wang, X.-X., Zhang, J., & Yu, M. (2019). Electrospinning. In B. Ding, X. Wang & J. Yu, (Eds.), *Electrospinning: Nanofabrication and applications* (1st ed.). Elsevier.
- Lopes, A. G. (2015). Single-use in the biopharmaceutical industry: A review of current technology impact, challenges and limitations. *Food and Bioproducts Processing*, 93, 98–114. <https://doi.org/10.1016/j.fbp.2013.12.002>
- Menkhaus, T. J., Varadaraju, H., Zhang, L., Schneiderman, S., Bjstrom, S., Liu, L., & Fong, H. (2010). Electrospun nanofiber membranes surface functionalized with 3-dimensional nanolayers as an innovative adsorption medium with ultra-high capacity and throughput. *Chemical Communications*, 46, 3720–3722. <https://doi.org/10.1039/c001802c>
- Metzger, K. F. J., Voloshin, A., Schillinger, H., Kühnel, H., & Maurer, M. (2020). Adsorptive filtration: A case study for early impurity reduction in an *Escherichia coli* production process. *Biotechnology Progress*, 36, e2948. <https://doi.org/10.1002/btpr.2948>
- Nadar, S., Somasundaram, B., Charry, M., Billakanti, J., Shave, E., Baker, K., & Lua, L. H. L. (2022). Design and optimization of membrane chromatography for monoclonal antibody charge variant separation. *Biotechnology Progress*, 38(6), 1–15. <https://doi.org/10.1002/btpr.3288>
- Najafi, M., Chery, J., & Frey, M. (2018). Functionalized electrospun poly(vinyl alcohol) nanofibrous membranes with poly(methyl vinyl ether-alt-maleic anhydride) for protein adsorption. *Materials*, 11(6), 1002. <https://doi.org/10.3390/ma11061002>
- Napoleone, A., Laurén, I., Linkgreim, T., Dahllund, L., Persson, H., Andersson, O., Olsson, A., Hultqvist, G., Frank, P., Hall, M., Morrison, A., Andersson, A., Lord, M., & Mangsbo, S. (2021). Fed-batch production assessment of a tetravalent bispecific antibody: A case study on piggyBac stably transfected HEK293 cells. *New Biotechnology*, 65, 9–19. <https://doi.org/10.1016/j.nbt.2021.07.002>
- Nevstrueva, D., Pihlajamäki, A., Nikkola, J., & Mänttari, M. (2018). Effect of precipitation temperature on the properties of cellulose ultrafiltration membranes prepared via immersion precipitation with ionic liquid as solvent. *Membranes*, 8(4), 87. <https://doi.org/10.3390/membranes8040087>
- Orr, V., Zhong, L., Moo-Young, M., & Chou, C. P. (2013). Recent advances in bioprocessing application of membrane chromatography. *Biotechnology Advances*, 31(4), 450–465. <https://doi.org/10.1016/j.biotechadv.2013.01.007>
- Pereira Aguilar, P., Reiter, K., Wetter, V., Steppert, P., Maresch, D., Ling, W. L., Satzer, P., & Jungbauer, A. (2020). Capture and purification of human immunodeficiency virus-1 virus-like particles: Convective media vs porous beads. *Journal of Chromatography A*, 1627, 461378. <https://doi.org/10.1016/j.chroma.2020.461378>
- Pinchuk, L. S., Goldade, V. A., Makarevich, A. V., & Kestelman, V. N. (2012). *Meltblowing techniques, Melt blowing equipment, technology, and polymer fibrous materials* (1st ed.). Springer. <https://doi.org/10.1007/978-3-642-55984-6>
- Pollard, D., Brower, M., Abe, Y., & Lopes, A. G. (2016). Standardized economic Cost modeling for next-generation mAb production. *Bioprocess International* (September).
- Pourdeyhimi, B., & Chappas, W. (2012). *High surface area fiber and textiles made from the same* (Patent No. 8,129,019). U.S. Patent and Trademark Office.
- Pourdeyhimi, B., Chappas, W., & Barnes, H. M. (2016). *Articles containing woven or non-ultra-high surface area macro polymeric fibers* (Patent No. 9,284,663). U.S. Patent and Trademark Office.
- Pourdeyhimi, B., Fedorova, N. V., & Sharp, S. R. (2013a). *High strength, durable micro and nano-fiber fabrics produced by fibrillating bicomponent islands in the sea fibers* (Patent No. 8,420,556 B2). U.S. Patent and Trademark Office.
- Pourdeyhimi, B., Fedorova, N. V., & Sharp, S. R. (2013b). *Micro and nanofiber nonwoven spunbonded fabric* (Patent No. 8,349,232 B2). U.S. Patent and Trademark Office.
- Pourdeyhimi, B., & Sharp, S. R. (2011). *High strength, durable fabrics produced by fibrillating multilobal fibers* (Patent No. 7,883,772 B2). U.S. Patent and Trademark Office.
- Rajesh, S., Crandall, C., Schneiderman, S., & Menkhaus, T. J. (2018). Cellulose-graft-polyethyleneamidoamine anion-exchange nanofiber membranes for simultaneous protein adsorption and virus filtration. *ACS Applied Nano Materials*, 1(7), 3321–3330. <https://doi.org/10.1021/acsnm.8b00519>
- Rajesh, S., Schneiderman, S., Crandall, C., Fong, H., & Menkhaus, T. J. (2017). Synthesis of cellulose-graft-polypropionic acid nanofiber cation-exchange membrane adsorbents for high-efficiency separations. *ACS Applied Materials & Interfaces*, 9(46), 41055–41065. <https://doi.org/10.1021/acsnm.7b13459>
- Rathore, A. S., Kumar, D., & Kateja, N. (2018). Recent developments in chromatographic purification of biopharmaceuticals. *Biotechnology Letters*, 40(6), 895–905. <https://doi.org/10.1007/s10529-018-2552-1>
- Romero, J. J., Jenkins, E. W., Osuofa, J., & Husson, S. M. (2023). Computational framework for the techno-economic analysis of monoclonal antibody capture chromatography platforms. *Journal of Chromatography A*, 1689, 463755. <https://doi.org/10.1016/j.chroma.2022.463755>
- Ruscic, J., Perry, C., Mukhopadhyay, T., Takeuchi, Y., & Bracewell, D. G. (2019). Lentiviral vector purification using nanofiber ion-exchange chromatography. *Molecular Therapy - Methods & Clinical Development*, 15(December), 52–62. <https://doi.org/10.1016/j.omtm.2019.08.007>
- Schwellenbach, J., Taft, F., Villain, L., & Strube, J. (2016). Preparation and characterization of high capacity, strong cation-exchange fiber based adsorbents. *Journal of Chromatography A*, 1447, 92–106. <https://doi.org/10.1016/j.chroma.2016.04.019>
- Shan, H., Wang, X., Shi, F., Yan, J., Yu, J., & Ding, B. (2017). Hierarchical porous structured SiO₂/SnO₂ nanofibrous membrane with superb flexibility for molecular filtration. *ACS Applied Materials & Interfaces*, 9(22), 18966–18976. <https://doi.org/10.1021/acsnm.7b04518>

- Sinclair, A., & Mange, M. (2009). Disposables cost contributions: A sensitivity analysis. *BioPharm International*, 22(4), 28–32.
- Singh, N., Arunkumar, A., Peck, M., Voloshin, A. M., Moreno, A. M., Tan, Z., Hester, J., Borys, M. C., & Li, Z. J. (2017). Development of adsorptive hybrid filters to enable two-step purification of biologics. *mAbs*, 9(2), 350–364. <https://doi.org/10.1080/19420862.2016.1267091>
- Soltani, I., & Macosko, C. W. (2018). Influence of rheology and surface properties on morphology of nanofibers derived from islands-in-the-sea meltblown nonwovens. *Polymer*, 145, 21–30. <https://doi.org/10.1016/j.polymer.2018.04.051>
- Son, M., Choi, H., Liu, L., Park, H., & Choi, H. (2014). Optimized synthesis conditions of polyethersulfone support layer for enhanced water flux for thin film composite membrane. *Environmental Engineering Research*, 19(4), 339–344. <https://doi.org/10.4491/eer.2014.045>
- Steel, D. (2022). Increasing processing efficiency, purity, and recovery of lentiviral particles for viral vector development. *Bioprocess International*, 20 (Nov-Dec).
- Sun, W., Liu, W., Wu, Z., & Chen, H. (2020). Chemical surface modification of polymeric biomaterials for biomedical applications. *Macromolecular Rapid Communications*, 41(8), 1900430. <https://doi.org/10.1002/marc.201900430>
- Trnovec, H., Doles, T., Hribar, G., Furlan, N., & Podgornik, A. (2020). Characterization of membrane adsorbents used for impurity removal during the continuous purification of monoclonal antibodies. *Journal of Chromatography A*, 1609, 460518. <https://doi.org/10.1016/j.chroma.2019.460518>
- Turnbull, J., Wright, B., Green, N. K., Tarrant, R., Roberts, I., Hardick, O., & Bracewell, D. G. (2019). Adenovirus 5 recovery using nanofiber ion-exchange adsorbents. *Biotechnology and Bioengineering*, 116, 1698–1709. <https://doi.org/10.1002/bit.26972>
- Van de Velde, J., Saller, M. J., Eyer, K., & Voloshin, A. (2020). Chromatographic clarification overcomes chromatin-mediated hitch-hiking interactions on protein A capture column. *Biotechnology and Bioengineering*, 117(11), 3413–3421. <https://doi.org/10.1002/bit.27513>
- Vogg, S., Pfeifer, F., Ulmer, N., & Morbidelli, M. (2020). Process intensification by frontal chromatography: Performance comparison of resin and membrane adsorbent for monovalent antibody aggregate removal. *Biotechnology and Bioengineering*, 117(3), 662–672. <https://doi.org/10.1002/bit.27235>
- Wang, L., Fu, Q., Yu, J., Liu, L., & Ding, B. (2019). Cellulose nanofibrous membranes modified with phenyl glycidyl ether for efficient adsorption of bovine serum albumin. *Advanced Fiber Materials*, 1, 188–196. <https://doi.org/10.1007/s42765-019-00010-1>
- Winderl, J., Neumann, E., & Hubbuch, J. (2021). Exploration of fiber-based cation exchange adsorbents for the removal of monoclonal antibody aggregates. *Journal of Chromatography A*, 1654, 462451. <https://doi.org/10.1016/j.chroma.2021.462451>
- Winderl, J., Spies, T., & Hubbuch, J. (2018). Packing characteristics of winged shaped polymer fiber supports for preparative chromatography. *Journal of Chromatography A*, 1553, 67–80. <https://doi.org/10.1016/j.chroma.2018.04.020>
- Wood, H., Wang, J., & Sourirajan, S. (1993). The effect of polyethersulfone concentration on flat and hollow fiber membrane performance. *Separation Science and Technology*, 28(15–16), 2297–2317. <https://doi.org/10.1080/01496399308019740>
- Yang, X., Merenda, A., AL-Attabi, R., Dumée, L. F., Zhang, X., Thang, S. H., Pham, H., & Kong, L. (2022). Towards next generation high throughput ion exchange membranes for downstream bioprocessing: A review. *Journal of Membrane Science*, 647, 120325. <https://doi.org/10.1016/j.memsci.2022.120325>
- Yi, S., Dai, F., Ma, Y., Yan, T., Si, Y., & Sun, G. (2017). Ultrafine silk-derived nanofibrous membranes exhibiting effective lysozyme adsorption. *ACS Sustainable Chemistry & Engineering*, 5(10), 8777–8784. <https://doi.org/10.1021/acssuschemeng.7b01580>
- Zhang, L., Menkhaus, T., & Fong, H. (2008). Fabrication and bioseparation studies of adsorptive membranes/felts made from electrospun cellulose acetate nanofibers. *Journal of Membrane Science*, 319(1–2), 176–184. <https://doi.org/10.1016/j.memsci.2008.03.030>
- Zhang, T., Wan, Y., Wang, Y., & Li, Y. (2021). Removing a single-arm species by fibro PrismA in purifying an asymmetric IgG-like bispecific antibody. *Protein Expression and Purification*, 182, 105847. <https://doi.org/10.1016/j.pep.2021.105847>
- Zheng, Y., Gurgel, P. V., & Carbonell, R. G. (2011). Effects of UV exposure and initiator concentration on the spatial variation of poly(glycidyl methacrylate) grafts on nonwoven fabrics. *Industrial & Engineering Chemistry Research*, 50(10), 6115–6123. <https://doi.org/10.1021/ie1021333>
- Zheng, Y., Liu, H., Gurgel, P. V., & Carbonell, R. G. (2010). Polypropylene nonwoven fabrics with conformal grafting of poly(glycidyl methacrylate) for bioseparations. *Journal of Membrane Science*, 364(1–2), 362–371. <https://doi.org/10.1016/j.memsci.2010.08.037>
- Zydney, A. L. (2021). New developments in membranes for bioprocessing: A review. *Journal of Membrane Science*, 620(October 2020), 118804. <https://doi.org/10.1016/j.memsci.2020.118804>

How to cite this article: Lavoie, J., Fan, J., Pourdeyhimi, B., Boi, C., & Carbonell, R. G. (2023). Advances in high-throughput, high-capacity nonwoven membranes for chromatography in downstream processing: A review. *Biotechnology and Bioengineering*, 1–18. <https://doi.org/10.1002/bit.28457>